Electronic Supplementary Information

Effects of aromatic spacers on film morphology and device memory performance based on imidazole-π-triphenylamine derivatives

Hao Zhuang, Qianhao Zhou, Qijian Zhang, Hua Li,* Najun Li, Qingfeng Xu and Jianmei Lu*

College of Chemistry, Chemical Engineering and Materials Science, Collaborative Innovation Center of Suzhou Nano Science and Technology, Soochow University, Suzhou 215123, China. E-mail: lujm@suda.edu.cn; Fax: +86 512 65880367; Tel: +86 512 65880368

1. NMR Spectra.

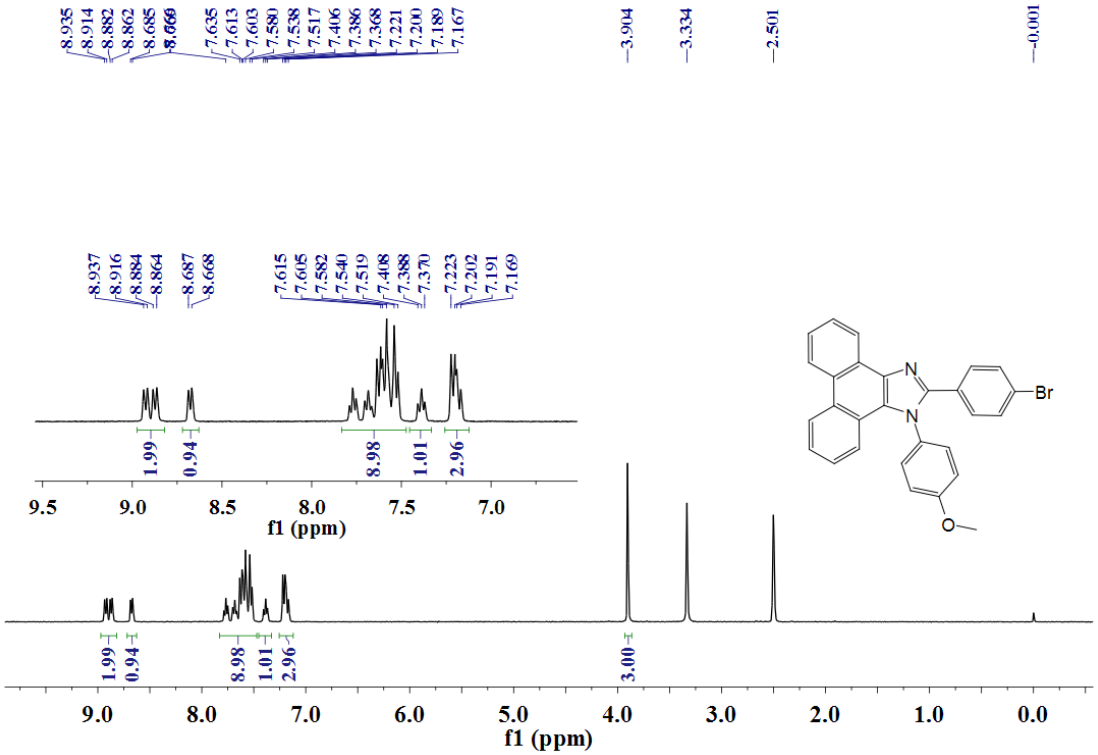

Figure S1. ^{1}H NMR spectrum of compound **1** in DMSO-d_6.

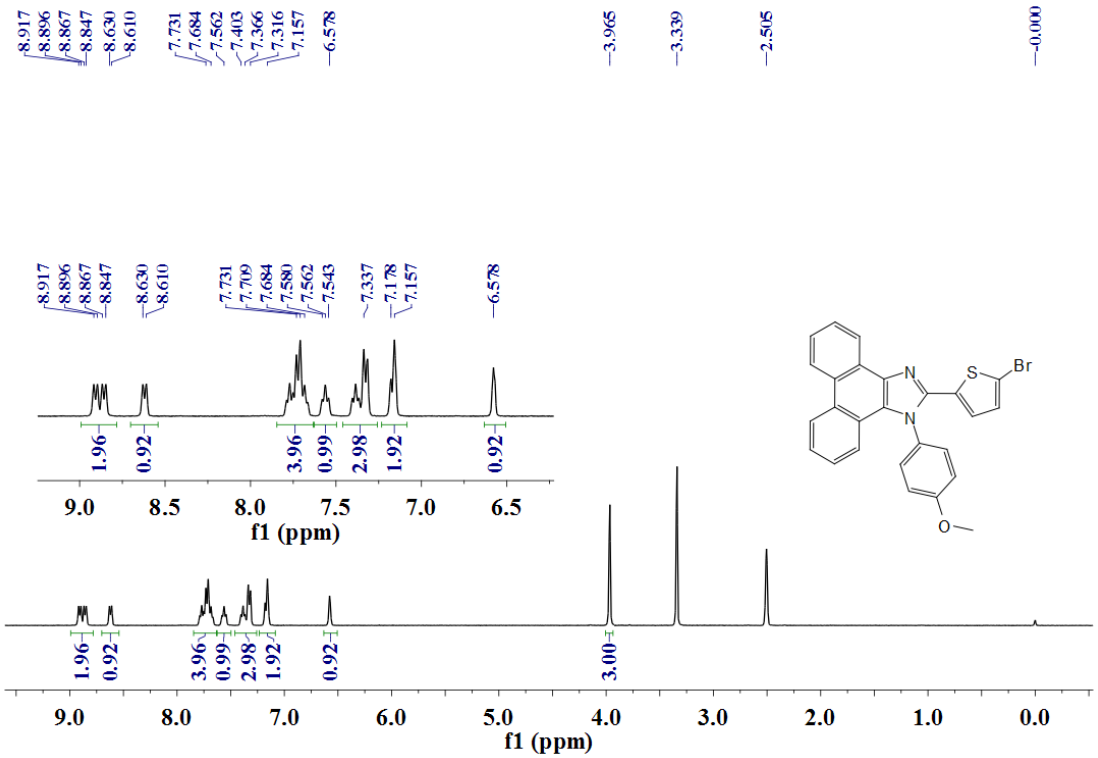

Figure S2. ^{1}H NMR spectrum of compound **2** in DMSO-d_6.

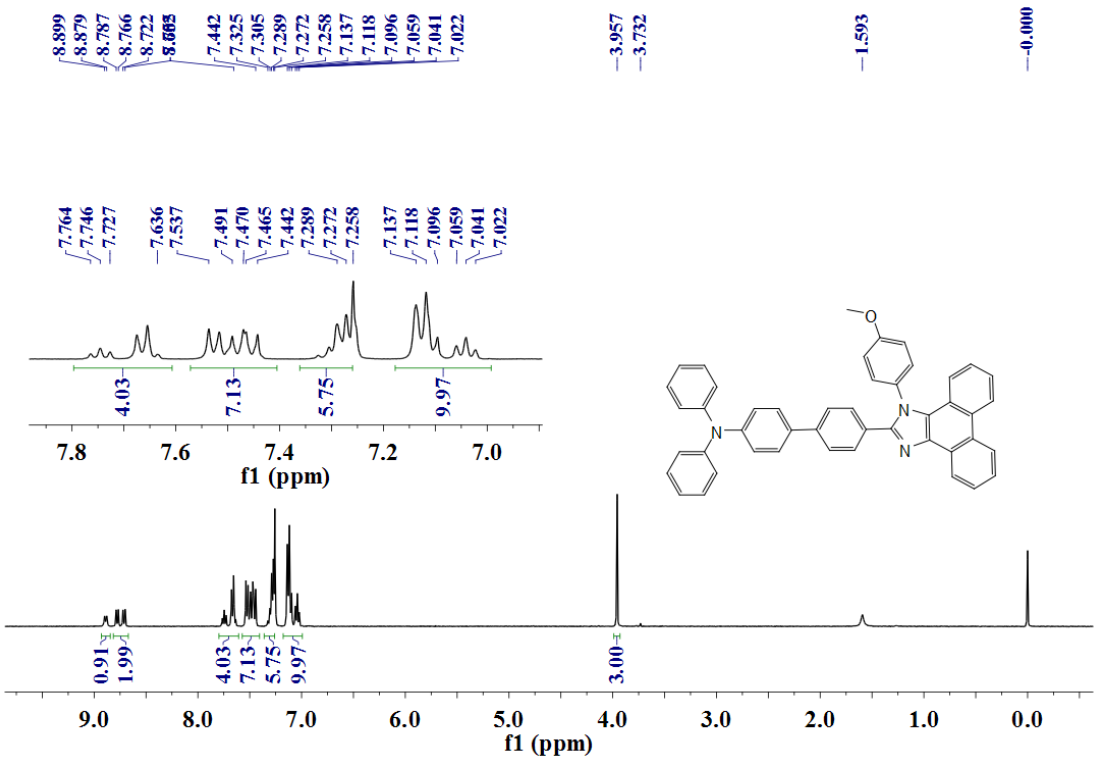

Figure S3. ^{1}H NMR spectrum of TPAPPI in $CDCl_3$.

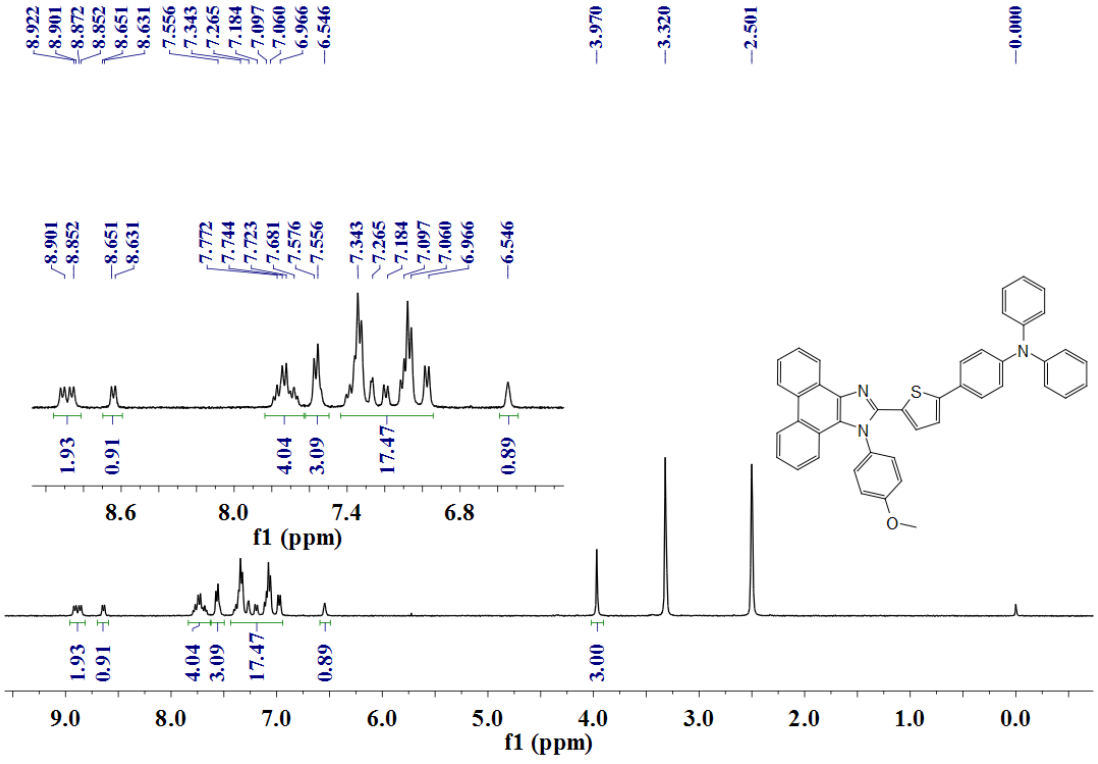

Figure S4. ^{1}H NMR spectrum of TPATPI in DMSO-d_6.

2. Cyclic Voltammogram of Ferrocene.

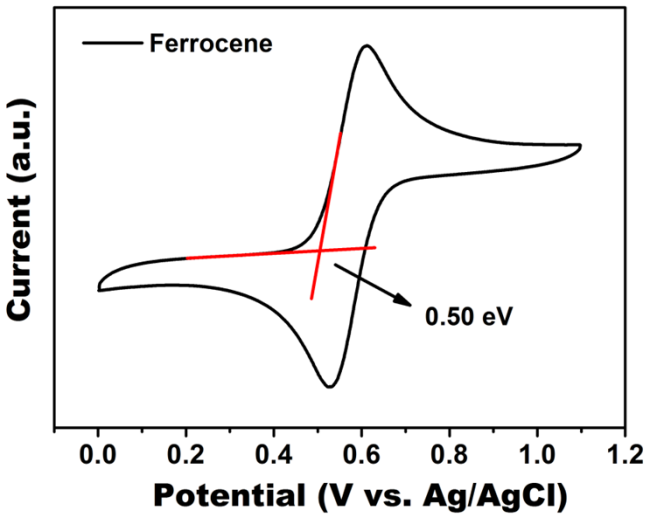

Figure S5. Cyclic voltammogram of the ferrocene standard in acetonitrile at the scan rate of 100 mV s^{-1}.

3. *I-V* curves with an embedded LiF buffering layer.

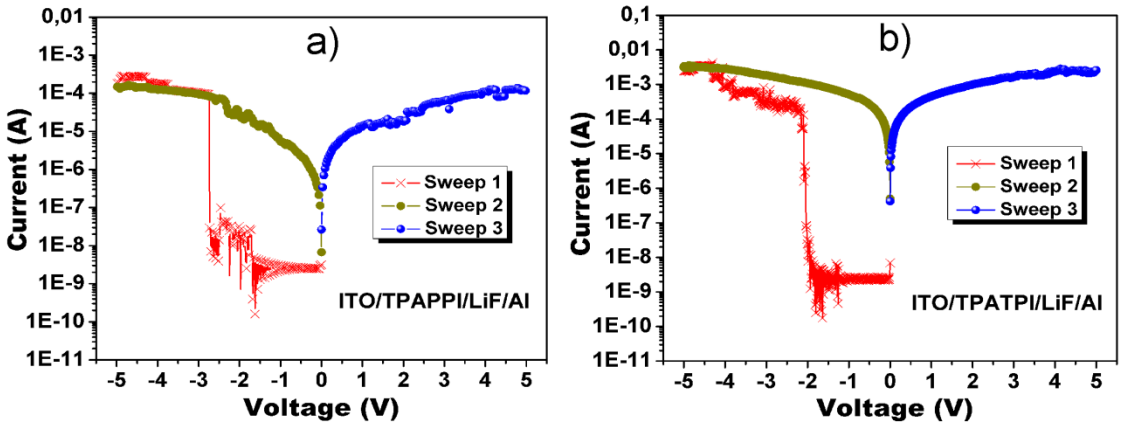

Figure S6. *I-V* characterization of the devices with the ITO/TPAPPI or TPATPI/LiF(5 nm)/Al structure.

4. *I-V* characterization of the devices based on different film thicknesses.

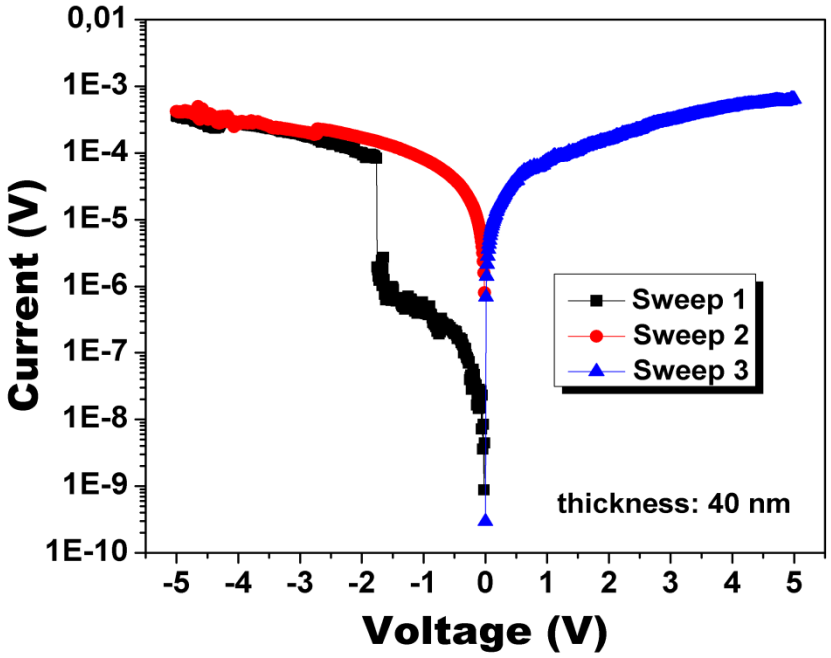

Figure S7. *I-V* characterization of the device based on a TPAPPI film thickness of 40 nm.

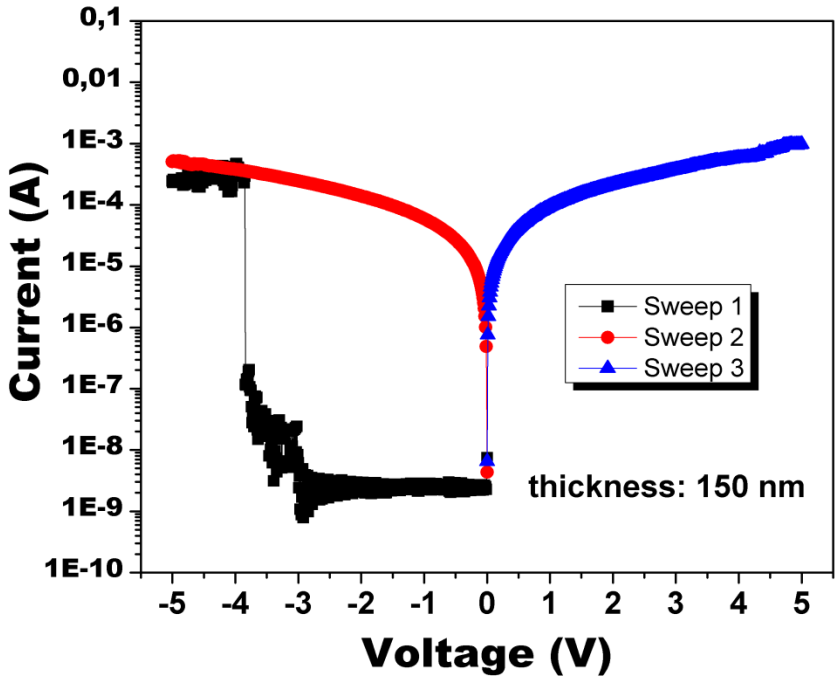

Figure S8. *I-V* characterization of the device based on a TPAPPI film thickness of 150 nm.

5. 3D-AFM Topography Images of the Thin Films before and after Annealing.

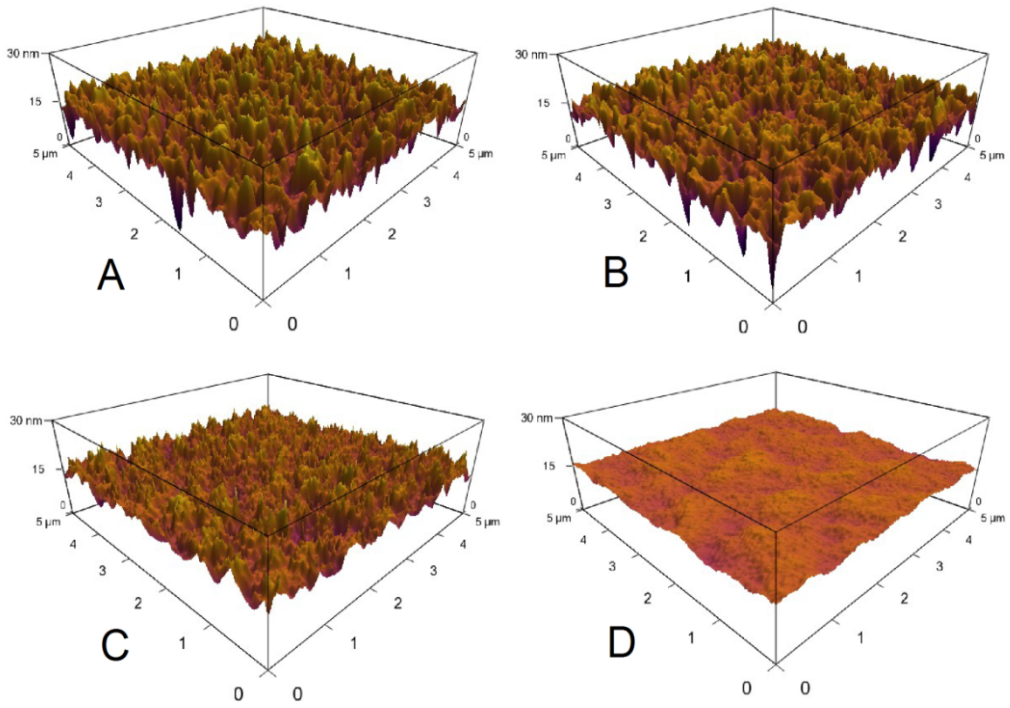

Figure S9. 3D-AFM topography images (5 × 5 μm^2) of TPAPPI (A,C) and TPATPI (B,D) films before (A,B) and after (C,D) annealing at 90 ^oC on ITO substrates.

6. Typical cross-section profiles of TPAPPI and TPATPI films.

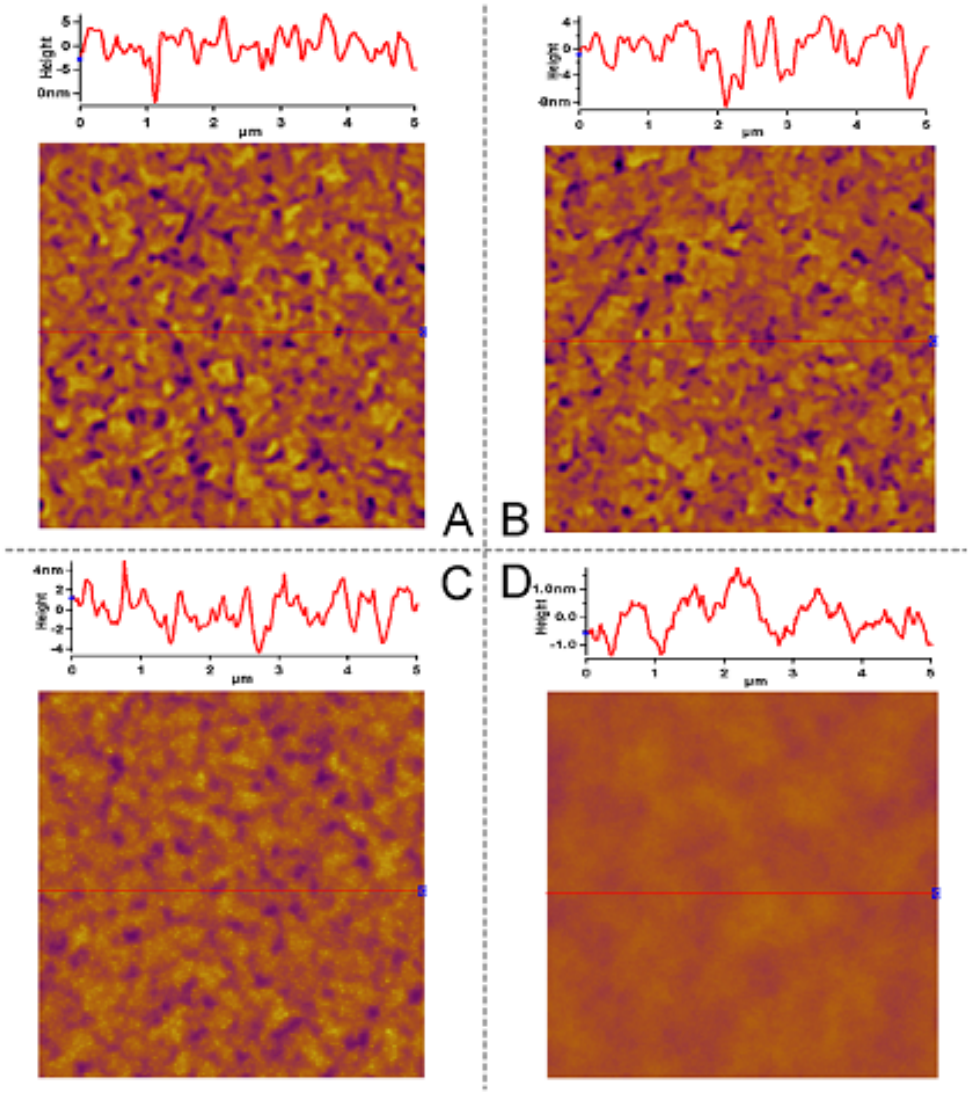

Figure S10. Typical cross-section profiles of TPAPPI (A,C) and TPATPI (B,D) films before (A,B) and after (C,D) annealing at 90 °C on ITO substrates obtained from AFM analysis.